RSC Advances

PAPER

View Article Online
View Journal | View Issue

Cite this: *RSC Adv.*, 2016, **6**, 93363

Ionomer-like structure in mature oil paint binding media†

Joen J. Hermans,*[a] Katrien Keune,[ab] Annelies van Loon,[a] Robert W. Corkery[c] and Piet D. Iedema[a]

Received 18th July 2016
Accepted 25th September 2016

DOI: 10.1039/c6ra18267d

www.rsc.org/advances

Infrared spectra of samples from oil paintings often show metal carboxylate bands that are broader and shifted compared to those of crystalline metal soap standards (metal complexes of long-chain saturated fatty acids). Using quantitative attenuated total reflection Fourier transform infrared spectroscopy (ATR-FTIR), it is demonstrated that the broad metal carboxylate band is typically too intense to be explained by carboxylates adsorbed on the surface of pigment particles or disordered metal complexes of saturated fatty acids. The metal carboxylate species associated with the broad bands must therefore be an integral part of the polymerized binding medium. Small-angle X-ray scattering (SAXS) measurements on model ionomer systems based on linseed oil revealed that the medium contains ionic clusters similar to more classical ionomers. These structural similarities are very helpful in understanding the chemistry of mature oil paint binding media and the potential degradation mechanisms that affect oil paintings.

1 Introduction

An oil paint is a mixture of pigments, a drying oil (triglycerides that have a high degree of unsaturation on their fatty acid chains) and a variety of possible additives. This mixture forms a complex heterogeneous system of solid particles suspended in a polymer matrix as it dries and ages through autoxidation. It is known that the common white pigments lead white ($2PbCO_3 \cdot Pb(OH)_2$) and zinc white (ZnO) easily release lead or zinc ions into the binding medium and that metal–carboxylate bonds (COOM) are often formed. These bonds are identified with Fourier transform infrared spectroscopy (FTIR) as strong asymmetric stretch vibration bands in de 1500–1600 cm^{-1} range. Previous studies on oil paint samples have shown that there are two distinct types of metal carboxylate species.[1–4] One type is characterized by sharp COOM bands that match pure references of crystalline metal complexes of saturated long-chain fatty acids, so-called metal soaps (*e.g.* at 1538 cm^{-1} for zinc complexes[5] and 1510 cm^{-1} with a shoulder at 1540 cm^{-1} for lead complexes[6]). Paintings conservators have linked the formation of these crystalline metal soaps in oil paints to cases of brittleness, transparency and delamination of paint layers, and especially lead soaps appear regularly as white spots on the exposed paint surface.[7–9] Because metal soaps are a widespread oil paint conservation issue, we have previously studied the crystallization of metal soaps from linseed oil to gain insight into the causes and kinetics of this process.[10]

The second type of metal carboxylate is associated with a much broader metal carboxylate band that is often shifted towards higher wavenumbers compared to the band maximum of crystalline metal soaps. While the two types may occur in relatively pure form, often a combination of the sharp and broad carboxylate band is observed in FTIR spectra of oil paint samples.[1,3] In an earlier paper, we have attempted to identify the second type of metal carboxylate.[4] It was demonstrated that the broad COOM band corresponds to an amorphous metal carboxylate species dispersed throughout the binding medium. Three types of amorphous metal carboxylate species were discussed:

(1) Carboxylate groups (mostly attached to the polymer network) adsorbed to the surface of pigment particles;

(2) Non-crystalline (disordered) metal complexes of fatty acids (possibly kinetically trapped in their amorphous state[10]);

(3) Metal ions bound to carboxylate functionalities on the polymerised oil network, a system similar to ionomers.

Though both carboxylates on the pigment surface[1,11] and ionomer structures[12–16] have been suggested by previous researchers as explanations for the broad COOM band, there is increasing evidence that an ionomer-like oil network is the dominant contributor to the broad metal carboxylate band in FTIR spectra. We have presented a novel route to synthesize ionomeric structures from linseed oil by co-polymerization with

[a]Van't Hoff Institute for Molecular Sciences, University of Amsterdam, PO box 94157, 1090GD Amsterdam, The Netherlands. E-mail: j.j.hermans@uva.nl; Tel: +31 20 525 6442

[b]Rijksmuseum Amsterdam, Conservation and Restoration, PO box 74888, 1070DN Amsterdam, The Netherlands

[c]KTH Royal Institute of Technology, Stockholm, SE 100 44, Sweden

† Electronic supplementary information (ESI) available: Composition of SAXS samples, ATR-FTIR spectra of various zinc white paints, derivation of relation between COOM/COOR ratio and pigment particle size and additional ATR-FTIR spectra of zinc and lead ionomers. See DOI: 10.1039/c6ra18267d

zinc sorbate, and it was shown that this material also has metal carboxylate features in FTIR spectra similar to the binding medium in zinc white paints.[4] Additionally, there is a striking similarity between COOM bands in FTIR spectra of commercial zinc-neutralized poly(ethylene-*co*-methacrylic acid) (pEMAA) ionomers and zinc white oil paint binding media.[17,18]

In this paper, we aim to prove that an ionomer-like state is indeed formed in the binding medium of oil paints when a broad metal carboxylate band is observed by quantifying the concentration of metal carboxylate groups with attenuated total reflection FTIR (ATR-FTIR). Additionally, we have used small angle X-ray scattering (SAXS) to compare the morphology of linseed oil-based ionomeric networks with more classical ionomers described in literature.

2 Experimental

2.1 Preparation of samples

Metal sorbate complexes were prepared by dissolving 550 mg sorbic acid (Aldrich, 99+%) with 1 mL triethylamine (Sigma-Aldrich, >99%) in 20 mL demineralized water at 50 °C. The addition of 1.0 g $Zn(NO_3)_2 \cdot 6H_2O$ (Sigma-Aldrich, p.a.) or 1.1 g $Pb(NO_3)_2$ (Sigma-Aldrich, >99%) dissolved in 5 mL water resulted in immediate precipitation of the white product. After stirring for 20 minutes, the product was separated by vacuum filtration, washed with water followed by acetone, and dried in a rotary evaporator under reduced pressure. The metal sorbate salts were stored under inert atmosphere and/or at low temperatures to avoid oxidation.

Ionomer samples for quantitative ATR-FTIR measurements were made by mixing 10, 15, 20, 25, 30, 35 or 40 mg zinc sorbate or lead sorbate with cold-pressed untreated linseed oil (Kremer Pigmente) to a total weight of 200 mg. The mixtures were ground to a smooth paste with a mortar and pestle, spread thinly on a glass slide, and cured overnight in an air-circulated oven at 150 °C. Metal concentrations for the lead ionomer samples were chosen lower than the zinc ionomers because higher concentrations led to sample mixtures that were too thick to be spread evenly. The samples for SAXS measurements were prepared in a similar fashion (exact composition of the samples is given in Table S1†).

Model paint mixtures were made by stirring 0.5 g ZnO (Sigma-Aldrich, p.a.) or 1.37 g PbO (Alfa Aesar, >99%) with 3 g cold-pressed untreated linseed oil and 1 mL demineralized water in a sealed vial for 3 days. After allowing the mixture to settle, a few drops of the oil layers were spread thinly on a glass slide and dried at room temperature. ATR-FTIR spectra of touch-dry samples were recorded after approximately 7 weeks.

2.2 Analysis

ATR-FTIR spectra of ionomers were measured on a Perkin Elmer Frontier FT-IR spectrometer equipped with a Pike diamond GladiATR module. Model paints were measured with a similar module on a Varian 660-IR FTIR spectrometer. In all cases, spectra were recorded at 4 cm^{-1} resolution and 16 scans. To account for potential sample inhomogeneity, five independent spectra were recorded on different sections of each sample. In Fig. 1, these spectra have been averaged to yield one spectrum per sample. For data analysis, each spectrum was treated separately and only the final band areas were averaged.

FTIR spectra were subjected to a tailored band integration algorithm using Wolfram Mathematica software. Each spectrum was corrected for baseline shifts and normalized to the peak maximum of the ester CO band at 1738 cm^{-1}. To isolate the metal carboxylate band, a Pearson type IV distribution[19] was used to fit the ester CO band which was subsequently subtracted from the spectrum. The resulting isolated metal carboxylate band was integrated over a fixed range (1500–1690 cm^{-1} and 1490–1670 cm^{-1} for zinc and lead ionomers, respectively). Finally, the band areas were averaged for each sample, and a linear least squares fit was applied to yield a relation between relative metal carboxylate band area and the COOM/COOR ratio derived from the composition of the samples. More detailed information on the band integration algorithm is available on request.

SAXS analyses were performed at the I911-4 SAXS end station at the now superseded Max II storage ring at the MAX-lab synchrotron facility in Lund, Sweden.[20] The I911 beamline contains a superconducting wiggler to produce a brilliance of 3 × 10^{15} photons/s/mrad^2/mm^2/0.1% bandwidth and an energy range of 7–18 keV. Monochromation and focusing was achieved *via* a curved Si(111) crystal and a Mo–Si multilayer mirror further downstream. The beam was collimated by two pairs of slits. The intensity of the incident (I_0) and transmitted (I_t) X-ray beam was monitored through a scintillator and a pin diode, respectively. The X-ray beam size incident on the sample was *ca.* 300 × 300 μm^2. Samples were mounted in holders with Kapton

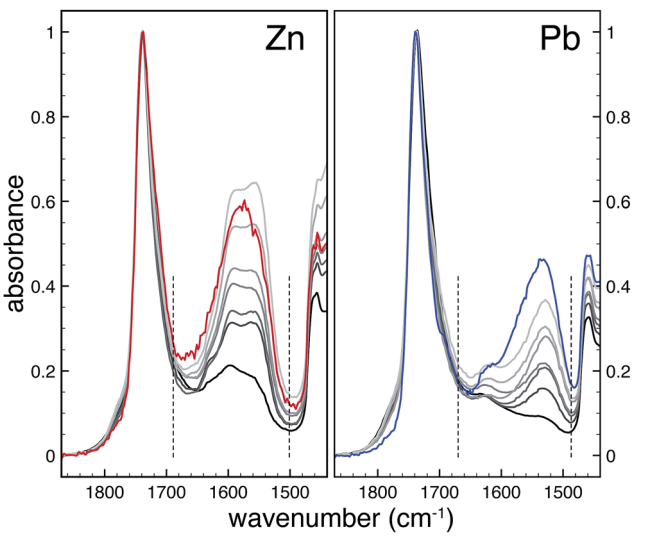

Fig. 1 ATR-FTIR spectra of Zn (left) and Pb (right) ionomers of linseed oil, normalized to the ester carbonyl band at 1738 cm^{-1}. The spectra from black to light grey range in relative concentration from 0.12–0.52 and 0.08–0.33 COOM/COOR for zinc and lead, respectively. The red and blue spectra are from model paints of ZnO or PbO in linseed oil, and all spectra are the average of 5 independent measurements. Dashed lines indicate the band integration limits used after ester CO band subtraction and spectral processing.

tape windows. Scattered X-rays were recorded using a Pilatus 1M 2D hybrid pixel detector. Silver behenate was used to calibrate the sample-to-detector distance, detector tilt and beam centre. Data sets including beam intensities, calibrants, samples and empty cells were reduced and analysed using the in-house software package bli9114. Full-circle radial integrations of the 2D measurements yielded 1D q *vs.* $I[q]$ data sets including background subtraction and intensity calibration as the final output. Measurements were performed using a wavelength of 0.9 Å and a sample-to-detector distance of *ca.* 1.9 m, corresponding to a q-range of 0.08 to 4 nm^{-1}. All samples were exposed for 5 minutes.

3 Results

3.1 Quantitative analysis of broad metal carboxylate bands

To determine the concentration of COOM groups in paint samples, we have used quantitative ATR-FTIR. Fig. 1 shows FTIR spectra of zinc and lead ionomers synthesized from a mixture of the metal sorbate and linseed oil with increasing concentrations of metal ions. Spectra were normalized to the ester CO band at 1738 cm^{-1}, effectively using it as an internal standard. Since we cannot directly measure the concentration of ester groups in paint samples, the derived concentration of COOM groups will be relative to the concentration of ester groups. The ester CO band was subtracted from the spectrum using a custom spectral processing algorithm, after which the isolated COOM band could be integrated. A linear relationship was found between the COOM band area and the ratio of COOM and ester groups (COOM/COOR), shown in Fig. 2 (R^2 = 0.965 and 0.975 for Zn and Pb, respectively), with a similar slope for zinc and lead ionomers.

Two spectra belonging to model 'paint' films prepared with ZnO or PbO cured as thin films at room temperature are also shown in Fig. 1 (weight ratio pigment to linseed oil R_{wt} = 0.17 and 0.46 for ZnO and PbO). Though the concentration of pigment in these model films was quite low, much lower than in common oil paint formulations, the broad COOM bands are very intense in both cases. Using the calibration line of Fig. 2, it was found that the bands correspond to a COOM/COOR ratio of 0.43 and 0.51 for the ZnO and PbO film, respectively, which is equal to roughly 1.5 COOM groups per triacylglyceride molecule. Broad COOM bands of similar or even higher intensity are routinely found in samples from paintings or paint models in literature.[2,4,21,22] For example, the broad COOM bands of three custom ZnO paints prepared in 1990 and a Windsor and Newton safflower oil zinc white paint film from 1978 described by Osmond and co-workers[1] correspond to COOM/COOR ratios ranging from 0.42 up to 1.09 (see ESI for ATR-FTIR spectra†).

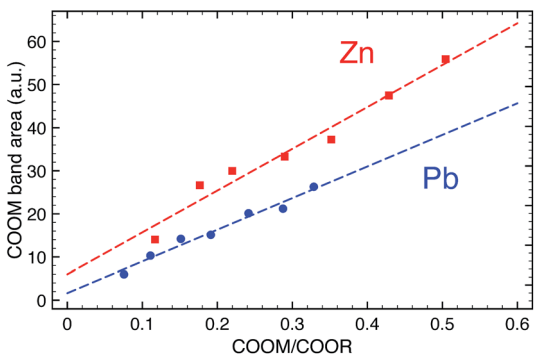

Fig. 2 Relation between COOM band area and COOM/COOR ratio for zinc (red squares) and lead (blue circles) ionomers. Standard errors in each point were smaller than the size of the symbol and the dashed lines are linear fits.

3.2 Carboxylates on the surface of pigment particles

Focusing on the pigment surface hypothesis, we can calculate the theoretical upper limit of COOM/COOR if all COOM bonds were located on the pigment surface using the following relation (see ESI for a full derivation†):

$$\left[\frac{[\mathrm{COOM}]}{[\mathrm{COOR}]}\right]_{\max} = R_{wt}\left(\frac{\rho_p N_A A_{COO} d_{part}}{2M_{w,LO}} - R_{wt}\right)^{-1}. \quad (1)$$

Here, R_{wt} is the weight ratio of pigment to oil, ρ_p is the density of the pigment, N_A is the Avogadro constant, A_{COO} is the surface area occupied by one carboxylate group, d_{part} is the average pigment particle diameter, and $M_{w,LO}$ is the average molecular mass of linseed oil. The main two assumptions in this relation are as follows:

- All particles are spherical and non-porous;[23]
- All carboxylate groups on the pigment surface are the result of ester hydrolysis, and therefore go at the expense of an ester group.

The second assumption is not likely to be true since carboxylate groups will also form through oxidation of unsaturated fatty acids, causing an overestimation of the maximum COOM/COOR ratio. However, not knowing the concentration of carboxylate groups formed through oxidation, the assumption is made to favor the pigment surface hypothesis.

Fig. 3 shows a plot of eqn (1) for ZnO in linseed oil as function of particle diameter d_{part} for different pigment to oil weight ratios R_{wt}, using a value of A_{COO} based on the dense packing of carboxylates in crystalline palmitic acid (23.3 $Å^2$).[24] The red curve corresponds to the pigment concentration of the model ZnO paint in Fig. 1 and the green curve is a plot for the approximate maximum pigment concentration of a typical artists' zinc white oil paint.[25] It is apparent that experimental COOM/COOR values (for instance, the red dashed line at COOM/COOR = 0.43 for our model ZnO paint) can only be reached with very small pigment particles, below 50 nm or smaller. Since ZnO particles used as pigment usually fall in the 0.5–3 μm range,[25] it is evident that, for a realistic paint formulation, there is not enough pigment surface area available for carboxylate groups to give rise to strong broad COOM bands.

In the context of the pigment surface explanation, it is worth mentioning that we have previously described a model ZnO paint film that during drying had formed a transparent ring consisting of only binding medium at the edge of the film.[4] ATR-FTIR spectra of samples taken from areas with and without zinc white pigment were nearly identical, both showing a strong

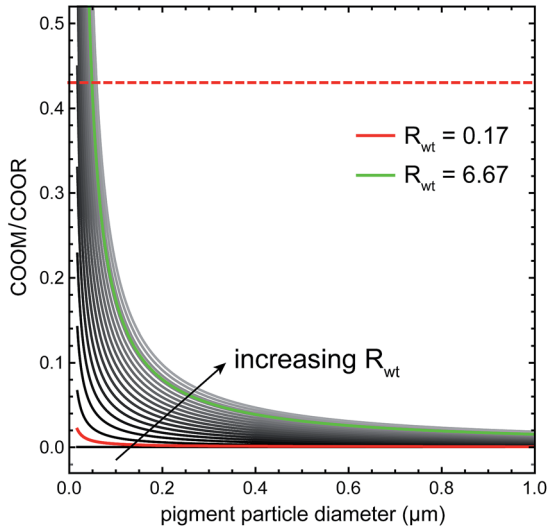

Fig. 3 The dependence of the maximum COOM/COOR ratio on particle size for various weight fractions of ZnO in linseed oil (grey lines), as described by eqn (1). The red curve corresponds to the ZnO model paint film of Fig. 1, where the top horizontal dashed line shows the experimental value of the COOM/COOR ratio in this system. The green curve corresponds to the maximum pigment concentration in a typical commercial zinc white oil paint.

broad COOM band, demonstrating that the pigment surface is probably not involved in the metal carboxylate species that causes the broad COOM band.

3.3 Amorphous metal soaps

We can use a similar quantitative line of reasoning to investigate the amorphous metal soaps explanation of broad COOM bands. Considering paint films that have fully dried (*i.e.* not longer containing unsaturations, like the model paint films shown in Fig. 1), the only carboxylic acids capable of forming amorphous metal soap complexes are the saturated fatty acids that are part of the total fatty acid side-chain composition of the drying oil and dicarboxylic acids that form during the autoxidative drying process. Both types of carboxylates are initially bound to the polymerized oil network through ester bonds, so a hydrolysis step is needed before metal soap complexes can be formed. Some cases have also been reported of modern oil paints where unoxidized oleic acid was present.[26] However, since this is not a very common observation and there seems to be no correlation between the detection of oleic acid and broad COOM bands, we assume that oleic acid does not generally play a role in metal soap formation.

In a typical linseed oil, saturated fatty acids account for about 7–13% of the total number of fatty acids present as triglycerides.[27] When we consider the, rather unrealistic, case that all saturated fatty acids have become available for metal binding through hydrolysis of their triglyceride ester bond while all other ester bonds connected to unsaturated fatty acids remain intact, the maximum ratio COOM/COOR is still limited to 0.075–0.15, depending on the exact saturated fatty acid content. Dicarboxylic acids formed through oxidation and subsequent hydrolysis may reasonably increase this maximum ratio to some extent. However, it remains highly unlikely in the amorphous metal soaps hypothesis that the COOM/COOR ratio approaches the typical experimental value of 0.43 or higher. Therefore, amorphous metal soaps will have at most a minor contribution to the broad COOM band observed in FTIR spectra, and the majority of carboxylate groups that give rise to a broad COOM band in zinc or lead containing oil paint must have formed through oxidation of the double bonds of linolenic, linoleic or oleic acid side-chains, or through hydrolysis of ester bonds with unsaturated fatty acids. In both cases, in a fully cured oil paint system these types of carboxylate groups will be covalently bound to the polymer network, which the formation of COOM groups has transformed to an ionomer-like structure.

3.4 Characterization of ionomer morphology by SAXS

Having shown that typical broad COOM bands in (model) oil paint samples are so strong that the large majority of these carboxylates *must* be part of the polymerized oil network, we will now focus on comparing the morphology of our ionomer system based on linseed oil and metal sorbate with more classical ionomers as described in literature. In turn, ionomer morphology may provide useful information on material properties concerning ion transport, molecular diffusion and mechanical flexibility. In SAXS profiles, ionomers typically exhibit a broad peak with a Bragg spacing d between 20–100 Å and an upturn at very small angles.[28] While the upturn is usually attributed to long-range inhomogeneities in the concentration of metal ions,[28,29] the broad peak is caused by clustering of ionic groups (metal carboxylate groups in the present case).[30,31] The concentration and size of ion-rich clusters generally depend on the metal ion species bound to the ionic groups[32] as well as the positions of pendant ionic groups and the architecture of the polymer matrix.[33]

Fig. 4 shows SAXS profiles of both zinc and lead ionomers as function of scattering vector q (where $q = 2\pi/d$), for two different total concentrations of carboxylate groups (molar ratio sorbate to linseed oil So/LO equal 0.6 and 1.1) and at different degrees of neutralization by zinc or lead ions (noted COO–Zn or COO–Pb in Fig. 4). ATR-FTIR spectra of these systems are shown in the ESI.† The zinc ionomers (Fig. 4a and b) show a characteristic ionomer peak with maxima close to $q = 0.9$ nm^{-1} ($d = 70$ Å) that increases in intensity with increasing metal content. The lead ionomers (Fig. 4c and d) only show an ionomer peak in the samples with the highest metal-content, with maxima at approximately $q = 0.7$ nm^{-1} ($d = 90$ Å). This observation of ionomer peaks in linseed oil co-polymerized with metal sorbates confirms that clusters rich in ionic groups have formed, and supports the assignment of the broad COOM band in FTIR spectra of oil paint samples to an ionomer-like state.

A scattering model was developed by Yarusso and Cooper[30] (YC), in which spherical clusters containing a high concentration of ionic groups are assumed to be distributed with liquid-like order and surrounded by a layer of immobile polymer matrix that limits the distance of closest approach between two ionic clusters. We have used a version of the YC model that

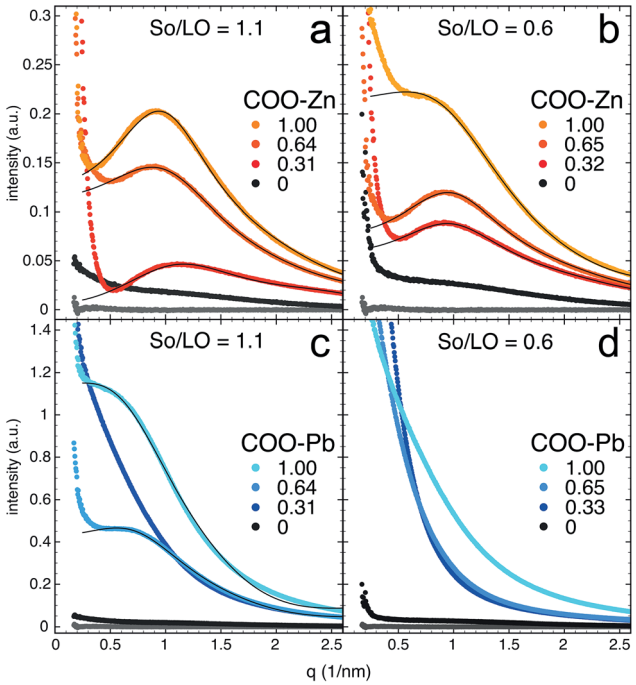

Fig. 4 SAXS profiles of (a and b) zinc and (c and d) lead ionomers prepared from linseed oil (LO), sorbic acid (So) and metal sorbate. So/LO refers to the molar ratio between sorbic acid ('free' and metal-bound combined) and linseed oil (*i.e.* the concentration of carboxylate groups). The numbers COO–Zn and COO–Pb refer to the fraction of the total sorbic acid groups bound to either zinc or lead (*i.e.* the metal ion concentration). Solid curves drawn through data points represent the best fits of the YC model described in eqn (2). The lowest grey profile in each plot corresponds to a pure linseed oil film, included for comparison.

groups all terms that contribute only to the intensity of the ionomer peak under a single parameter A and adds a constant C to account for variations in background intensity.[31] The resulting model is as follows:

$$I[q] = A\frac{{v_1}^2\Phi^2[qR_1]}{v_p + 8v_{CA}\Phi[2qR_{CA}]} + C, \quad (2)$$

in which

$$\Phi[x] = \frac{3(\sin x - x\cos x)}{x^3} \quad (3)$$

$$v_1 = \frac{4\pi {R_1}^3}{3} \quad (4)$$

$$v_{CA} = \frac{4\pi {R_{CA}}^3}{3}. \quad (5)$$

Here, $I[q]$ is the intensity of the signal as function of the scattering vector q, R_1 is the radius of an ionic cluster, R_{CA} is the radius of an ionic cluster including immobile polymer shell, and v_p is the sample volume occupied by one ionic cluster. The solid lines in Fig. 4 represent fits of the YC model to the scattering data excluding the low-angle upturn, which match the experimental data reasonably well even for these highly cross-linked polymer systems. Values for the radius of ionic clusters

Table 1 Fitted parameters of the YC model of eqn (2) to the scattering profiles of linseed oil ionomers shown Fig. 4a–c. So/LO and COO–M refer to the carboxylate concentrations and degree of metal neutralization noted in Fig. 4. Standard deviations in all fit parameters were 1% or lower

Ionomer	So/LO	COO–M	R_1 (nm)	R_{CA} (nm)	v_p (nm^3)
Zn	1.1	0.31	0.53	2.30	589
	1.1	0.64	1.34	2.41	598
	1.1	1.00	1.31	2.55	468
	0.6	0.32	1.21	2.53	553
	0.6	0.65	1.26	2.53	495
	0.6	1.00	1.45	2.45	1336
Pb	1.1	0.64	1.66	3.08	2373
	1.1	1.00	1.78	3.50	7681

R_1, the radius of ionic clusters including the immobile polymer layer R_{CA} and the volume of polymer medium occupied by one ionic cluster v_p for all samples that contained a ionomeric peak are shown in Table 1.

Interestingly, the size of ionic domains was only weakly influenced by the concentration of metal ions or the degree of neutralization. A similar observation has been made for zinc-neutralized poly(ethylene-*co*-acrylic acid) (pEAA) and sulfonated polystyrene ionomers (SpS).[33,34] With the exception of one zinc ionomer sample with intermediate metal concentration, radii of ionic clusters in the linseed oil zinc ionomers were in the range of 1.21–1.45 Å and cluster sizes including polymer shell were roughly twice as large at 2.30–2.45 Å. The radii of these ionic clusters are a factor of 2–3 larger than those reported for zinc-neutralized pEAA and SpS ionomers. While the intensity of the ionomeric peak clearly increases, no clear trend could be observed in the concentration of ionic clusters. Fitted values of v_p were mostly in the range of 500–600 nm^3 in these zinc ionomers.

The lead ionomers of linseed oil (Fig. 4c and d) differ significantly from the zinc ionomers. Only the two systems with highest lead concentration exhibit ionic clustering, while samples with lower metal concentration merely present evidence of inhomogeneity on a decreasing characteristic length scale with increasing lead concentration.[28] In the two samples with an ionomeric peak, the ionic domains are slightly larger than in their zinc ionomer counterparts (R_1 = 1.66 and 1.78 nm^3 and R_{CA} = 3.08 and 3.50 nm^3), and the concentration of ionic groups is significantly lower with $v_p = 2.4 \times 10^3$ and 7.7×10^3 nm^3. These values suggest that in lead ionomers of linseed oil, most lead ions do not reside in spherical ionic clusters but are distributed throughout the material with some long-scale inhomogeneity.

The observation that R_{CA} values are roughly twice as large as R_1 in linseed oil-based ionomers containing zinc or lead points to a relatively thick immobile polymer shell around the ionic clusters,[30,35] which is in agreement with the highly cross-linked and constrained nature of polymerized linseed oil.

4 Discussion

The significant differences that were found in the size and concentration of ionic clusters in zinc and lead ionomers might be related to effect the metal ions have on the polymerization of

linseed oil.[36] It is well known, for instance, that lead ions catalyze some of the oxidative polymerization reactions during drying, which could lead to a more cross-linked and more rigid oil network that hinders the formation of metal-rich clusters in the case of lead ionomers. Alternatively, the different preferred carboxylate coordination geometries for lead and zinc ions could play a role in the degree of cluster formation. Though these preliminary results on the size and concentration of ionic clusters in linseed oil-based ionomers already present useful information on the morphology of these systems, more detailed studies investigating the ionic cluster properties as function of temperature and/or solvent swelling on samples with a broader metal concentration range are needed to fully understand the significance of these results.

While we have shown that saturated fatty acids can only account for a small fraction of the broad COOM band observed in FTIR spectra of oil paint samples, it is important to note that carboxylate groups of saturated fatty acids may still participate in ionic clustering in linseed oil-based ionomers. If the concentration of free fatty acids remains low, it is presumed that they could remain homogeneously dispersed within the polymer network, making their behavior virtually indistinguishable from carboxylate functionalities attached covalently to the polymer network.

The presented evidence that the aged binding medium in many oil paints has important structural similarities to commercial well-studied ionomers is helpful in our understanding of the properties and degradation mechanisms of mature oil paints. For instance, it is expected that metal ions may migrate through the polymer medium with a similar 'ion-hopping' mechanism[37] as is described for pEMAA[38] and polyether-ester-sulfonate co-polymers.[39] This process is strongly influenced by the degree of mobility of the polymer segments. If the presence of lead ions really leads to a more cross-linked polymer medium compared to zinc ionomers, we may expect the metal ion mobility to be affected. However, the mobility of metal ions is also likely to depend on the mass of the specific metal ion, the strength of the COO–M bond and the homogeneity of the metal ion distribution in the polymer medium. Conductivity measurements of linseed oil-based ionomers could be employed to investigate the relative influence of these factors. Additionally, like all polymers, linseed oil networks feature a glass transition temperature (T_g), above which the mobility of polymer segments increases significantly. A dynamic mechanical analysis (DMA) study by Phenix reports broad thermal transitions for a variety of fully dried oil paints with values for T_g ranging from -2 to 45 °C, though some zinc white paints only showed gradual thermal softening in the investigated temperature range.[40] Further investigations linking thermal analysis methods to conductivity measurements should reveal the correlation between the glass transition and ion mobility in oil paint systems.

Our findings also have important implications for our understanding of metal soap formation in oil paints. We have shown that many oil paint layers apparently have a significant concentration of zinc or lead ions throughout the paint layer without forming crystalline metal soaps (yet). This situation suggests that the partial breakdown of pigments and release of ions is not a sufficient condition for crystalline metal soap formation. Neither does metal soap formation necessarily have to occur close to pigment particles when metal ions are spread throughout a paint layer. Instead, we hypothesize that the presence of a threshold concentration of free saturated fatty acids—once 'liberated' by hydrolysis of ester bonds—is a trigger for metal soap crystallization, having shown previously that the complexes of lead and zinc with palmitic acid are practically insoluble in linseed oil.[10] The formation of crystalline metal soap phases from linseed oil-based ionomers will be the topic of a forthcoming publication.

5 Conclusions

Two types of metal carboxylate asymmetric stretch vibration bands can be distinguished in FTIR spectra of oil paint samples: sharp well-defined (sets of) bands corresponding to crystalline metal soaps of saturated fatty acids, and broader bands (often shifted to higher wavenumbers) previously linked to an amorphous metal soap species. Employing a tailored model system of linseed oil co-polymerized with metal sorbates that shows the same broad metal carboxylate band, it is now possible to quantify the concentration of metal carboxylates relative to the concentration of ester bonds using standard ATR-FTIR. With this method, we have demonstrated that disordered complexes of metal ions and saturated fatty acids or carboxylates adsorbed on the surface of pigment particles can only account for a minor fraction of the amorphous metal carboxylate species commonly found in oil paint samples. Therefore, we conclude that, whenever a prominent broad metal carboxylate band is observed in FTIR spectra of oil paint samples, an ionomer-like binding medium has formed where metal ions bound to carboxylate groups covalently part of the oil network are dispersed throughout the medium.

Analysis with SAXS has shown that linseed oil-based ionomers prepared with zinc or lead contain clusters of ionic groups, which is an important structural similarity to more classical ionomer system described in literature. This result indicates that the body of research available on ionomers may be of great help to understand the properties and degradation mechanisms in mature oil paints. In the context of the problem of metal soap formation, it will be of special interest to study the transport of metal ions and fatty acids as function of temperature, humidity or degree of solvent swelling to assess the impact of storage and cleaning procedures on the degradation of oil paints.

Acknowledgements

The authors wish to thank Ana Labrador for her assistance during SAXS measurements at the I911-4 beamline at MAX-lab in Lund, Sweden and Gillian Osmond for useful discussions and her kind sharing of raw FTIR data. This work is part of the PAinT project, supported by the Science4Arts program of the Dutch Organization for Scientific Research (NWO), and the leadART project, part of the Joint Program Initiative for Joint Research Projects on Cultural Heritage (JPI-JHEP).

References

1 G. Osmond, J. J. Boon, L. Puskar and J. Drennan, *Appl. Spectrosc.*, 2012, **66**, 1136–1144.
2 Z. Kaszowska, K. Malek, M. Pańczyk and A. Mikołajska, *Vib. Spectrosc.*, 2013, **65**, 1–11.
3 L. Monico, K. Janssens, M. Cotte, L. Sorace, F. Vanmeert, B. G. Brunetti and C. Miliani, *Microchem. J.*, 2016, **124**, 272–282.
4 J. J. Hermans, K. Keune, A. van Loon and P. D. Iedema, *J. Anal. At. Spectrom.*, 2015, **30**, 1600–1608.
5 T. Ishioka, K. Maeda, I. Watanabe, S. Kawauchi and M. Harada, *Spectrochim. Acta, Part A*, 2000, **56**, 1731–1737.
6 J. Catalano, A. Murphy, Y. Yao, G. P. A. Yap, N. Zumbulyadis, S. A. Centeno and C. Dybowski, *Dalton Trans.*, 2015, **44**, 2340–2347.
7 C. Higgit, M. Spring and D. Saunders, *Technical Bulletin*, 2003, **24**, 75–95.
8 M. Plater, B. De Silva, T. Gelbrich, M. B. Hursthouse, C. L. Higgitt and D. R. Saunders, *Polyhedron*, 2003, **22**, 3171–3179.
9 K. Keune and J. Boon, *Stud. Conserv.*, 2007, **52**, 161–176.
10 J. Hermans, K. Keune, A. van Loon and P. Iedema, *Phys. Chem. Chem. Phys.*, 2016, **18**, 10896–10905.
11 C. Clementi, F. Rosi, A. Romani, R. Vivani, B. G. Brunetti and C. Miliani, *Appl. Spectrosc.*, 2012, **66**, 1233–1241.
12 J. van den Berg, K. van den Berg and J. Boon, *Prog. Org. Coat.*, 2001, **41**, 143–155.
13 J. van der Weerd, A. van Loon and J. J. Boon, *Stud. Conserv.*, 2005, **50**, 3–22.
14 C. S. Tumosa, D. Erhardt, M. F. Mecklenburg and X. Su, *Materials Research Society Symposium Proceedings*, 2005, pp. 25–31.
15 J. J. Boon, F. Hoogland and K. Keune, *AIC annual meeting*, Providence, Rhode Island, 2006, pp. 18–25.
16 A. Doménech-Carbó, M. T. Doménech-Carbó and X. Mas-Barberá, *Talanta*, 2007, **71**, 1569–1579.
17 M. Coleman, J. Lee and P. Painter, *Macromolecules*, 1990, **23**, 2339–2345.
18 T. Ishioka, *Polym. J.*, 1993, **25**, 1147–1152.
19 H. Keles, A. Naylor, F. Clegg and C. Sammon, *Analyst*, 2014, **139**, 2355–2369.
20 A. Labrador, Y. Cerenius, C. Svensson, K. Theodor and T. Plivelic, *J. Phys.: Conf. Ser.*, 2013, **425**, 072019.
21 K. Keune and G. Boevé-jones, *Issues in Contemporary Oil Paint*, 2014, pp. 283–294.
22 G. Osmond, B. Ebert and J. Drennan, *AICCM Bulletin*, 2014, **34**, 4–14.
23 The non-porosity of the ZnO used here was verified with N_2-physisorption, showing a BET surface area of 10.2 $m^2\ g^{-1}$. Using average particle sizes observed with SEM, this surface area is in the right range for non-porous spherical particles.
24 E. Moreno, R. Cordobilla, T. Calvet, F. J. Lahoz and A. I. Balana, *Acta Crystallogr., Sect. C: Cryst. Struct. Commun.*, 2006, **62**, o129–o131.
25 H. Kühn, in *Artists' Pigments*, ed. R. Feller, Cambridge University Press, 1986, vol. 1, pp. 169–186.
26 D. Rogala, S. Lake, C. Maines and M. Mecklenburg, *J. Am. Inst. Conserv.*, 2013, **49**, 96–113.
27 J. D. J. van den Berg, N. D. Vermist, L. Carlyle, M. Holčapek and J. J. Boon, *J. Sep. Sci.*, 2004, **27**, 181–199.
28 Y. S. Ding, S. R. Hubbard, K. O. Hodgson, R. A. Register and S. L. Cooper, *Macromolecules*, 1988, **21**, 1698–1703.
29 D. Wu, J. Phillips, R. Lundberg, W. Macknight and B. Chu, *Macromolecules*, 1989, **22**, 992–995.
30 D. J. Yarusso and S. L. Cooper, *Macromolecules*, 1983, **16**, 1871–1880.
31 N. M. Benetatos, C. D. Chan and K. I. Winey, *Macromolecules*, 2007, **40**, 1081–1088.
32 D. S. Bolintineanu, M. J. Stevens and A. L. Frischknecht, *Macromolecules*, 2013, **46**, 5381–5392.
33 M. E. Seitz, C. D. Chan, K. L. Opper, T. W. Baughman, K. B. Wagener and K. I. Winey, *J. Am. Chem. Soc.*, 2010, **132**, 8165–8174.
34 A. M. Castagna, W. Wang, K. I. Winey and J. Runt, *Macromolecules*, 2011, **44**, 2791–2798.
35 D. Yarusso and S. Cooper, *Polymer*, 1985, **26**, 371–378.
36 R. van Gorkum and E. Bouwman, *Coord. Chem. Rev.*, 2005, **249**, 1709–1728.
37 L. M. Hall, M. J. Stevens and A. L. Frischknecht, *Macromolecules*, 2012, **45**, 8097–8108.
38 N. Tierney and R. Register, *Macromolecules*, 2002, **35**, 2358–2364.
39 G. J. Tudryn, M. V. O'Reilly, S. Dou, D. R. King, K. I. Winey, J. Runt and R. H. Colby, *Macromolecules*, 2012, **45**, 3962–3973.
40 A. Phenix, *AIC Paintings Specialty Group Postprints*, 2009, vol. 22, pp. 72–89.